

A SYSTEMATIC METHOD FOR DETERMINING THE CONTROLLER GAINS IN A MULTI-SPAN WEB LINE

By

Benjamin D. Reish and Karl N. Reid
Oklahoma State University
USA

ABSTRACT

A web line may have multiple locations where feedback systems are used to control web and roller speeds, and web tension. The Euclid Web Line (EWL) in the Web Handling Research Center at Oklahoma State University is such a line. The EWL has four sections – unwind, S-wrap, process, and rewind section. The S-wrap establishes the web speed. There are five speed controllers and two tension controllers. For the studies reported in this paper, all controllers are assumed to be Proportional (P) + Integral (I) controllers. A systematic method for finding the controller gains is the primary objective of this paper. The method involves first simplifying the model for each section using a Routh Approximation, and then determining the controller gains based on selected performance criteria. Experimental studies on the Euclid line with the determined gains are presented.

NOMENCLATURE

A	-	Cross-sectional area of the web (width×thickness)
B_{fn}	-	Bearing friction
C_{pn}	-	Dancer torsional damping constant
C_{mn}	-	Motor damping
E	-	Young's Modulus
f_{qn}	-	Dancer input torque
GR_n	-	Gear Ratio between motor and shaft in contact with the web (number of shaft rotations per motor rotation)
J_{mn}	-	Motor Inertia
J_n	-	Combined inertia of the wound web, shaft, and the motor inertia reflected through the gear ratio
J_{pn}	-	Dancer arm inertia
J_{sn}	-	Inertia of the shaft the web is wound on

K_{is}	-	Integral gain for speed loop
K_{it}	-	Integral gain for tension loop
K_{mn}	-	Motor constant (torque per amp supplied current)
K_{pn}	-	Dancer torsional spring constant
K_{ps}	-	Proportional gain for speed loop
K_{pt}	-	Proportional gain for tension loop
k_r	-	Real root multiplier in third-order characteristic equations where they are defined as a real root and a second-order dynamic system
L_{arm}	-	Dancer arm length
L_n	-	Free span length
l_{cg}	-	Dancer center of gravity location from pivot
M_d	-	The set of denominator polynomial coefficients produced by the Routh Approximation method
M_n	-	The set of numerator polynomial coefficients produced by the Routh Approximation method
m_p	-	Dancer pendulum mass
n	-	Index number
R_n	-	Roller or roll radius
s	-	Laplace operator
$T_n(s)$	-	Web span tension in the Laplace domain
t_n	-	Tension in the web span
t_r	-	Rise time of a second-order dynamic system
$U_n(s)$	-	Current Input to the motor in the Laplace domain
u_n	-	Current Input to the motor
$V_n(s)$	-	Roller speeds in Laplace domain
$V_{n,0}$	-	Roller steady-state speeds
v_n	-	Roller speeds
$\Gamma(s)$	-	Dancer position in Laplace domain
γ	-	Dancer position
ζ	-	Damping ratio of a second-order dynamic system
ω_n	-	Motor rotation rate
ω_{nat}	-	Natural frequency of a second-order dynamic system
$\Omega(s)$	-	Motor rotation rate in Laplace domain

INTRODUCTION

Feedback systems are used in web lines to accurately control motor speeds and tensions. If these systems are not properly designed or tuned, and not independent, tension may not be controlled adequately [1]. The results may be web breakage, web slackness, overstretching, wrinkling, printing errors, lamination curling, loss of traction, sluggish operation, and web tension fluctuations and instabilities. Accuracy of tension control in a coating line is one example of a particularly serious case. Accurate tension control without tension fluctuations is often essential to evenness and quality of coating. Properly designed feedback systems may also be essential to running a line faster when profitability demands the use of thinner and thinner web materials and running different materials through the same line. Proper design of the feedback systems often starts with good modeling and simulation before “flying” the system. But solutions to two major problems must be addressed: (i) how to select the gains for each independent control system and (ii) what performance criteria should be used to guide the selection of gains.

This paper proposes a systematic method for selection of the gains, and a pairing with performance criteria that are easy to use.

Tension control has been the subject of many papers over the years. Only a few early papers are cited here, and these have been cited in most papers that have followed. Campbell developed a dynamic model for tension in a web assuming small strains and Hooke's Law, and discussed several methods of tension control when a web is transported [2]. King modeled a small portion of a newspaper press (roller, web span, nip) assuming a linear elastic web, and demonstrated that an unbalance in the roller results in oscillations of tension in the web span, the magnitude being dependent on the web speed [3]. Grenfell modeled a simple nipped roller- web span-nipped roller system and showed the effects of disturbances in the roller speeds on the tension in the web [4]. Brandenburg developed dynamic models that take into account spatial variations of parameters to analyze web lines where print registration is critical [5]. Shelton developed models for use in web tension control, and compared two methods of tension control - torque control and velocity control of a roller or rewinding roll of material [6]. Shin developed the concept of "primitive elements" in a web line, and used them to model web lines [7].

Reid and Shin considered the rewind of a web line where the motor drives the plant directly, and demonstrated that a web line that uses variable gain PID controller may have superior performance to a line with fixed gain controllers when there are significant time varying parameters [8]. A simplified model of the hypothetical system is a third order linear differential equation, which makes it straight forward to estimate gains based on a performance factor involving natural frequency and damping ratio.

Few of these papers focus on methods to determine controller gains, specifically. In general, there are two types of control systems used in most web lines - Speed Control and Tension Control. In the Euclid Web Line (schematic in Figure 1), the S-wrap rolls and the pull roll are under pure speed control, while the controllers for the unwind and rewind rolls use both speed control and tension control. Figure 2 shows a speed-based web tension control system with load cell feedback that can be used at either or both the unwind and rewind. An inner loop provides velocity control of the unwind roll (or rewind roll), and an outer tension loop that provides a correction to the speed reference [9]. Figure 3 shows a speed-based web tension control system with dancer position feedback instead of load cell feedback [9], that can be used at either or both the unwind and rewind. One configuration of the Euclid Line uses a speed-based tension control with load cell feedback at both the unwind and rewind. Another configuration uses a speed-based web tension control system with dancer position feedback at the unwind, and a speed-based system with load-cell feedback at the rewind.

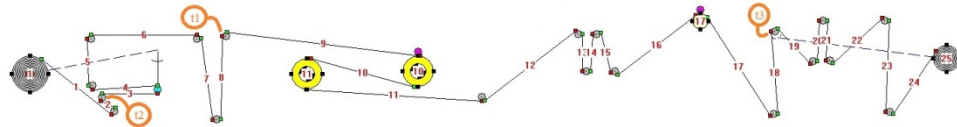


Figure 1 – The Euclid Web Line with rollers and spans numbered. The load cell locations are indicated with orange circles.

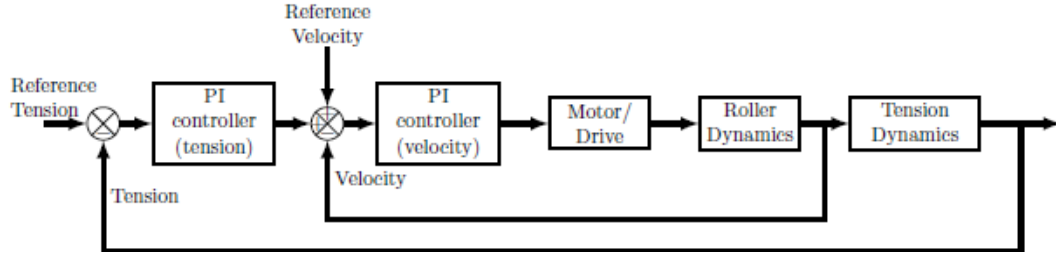


Figure 2 – Speed based web tension control system using load cell feedback

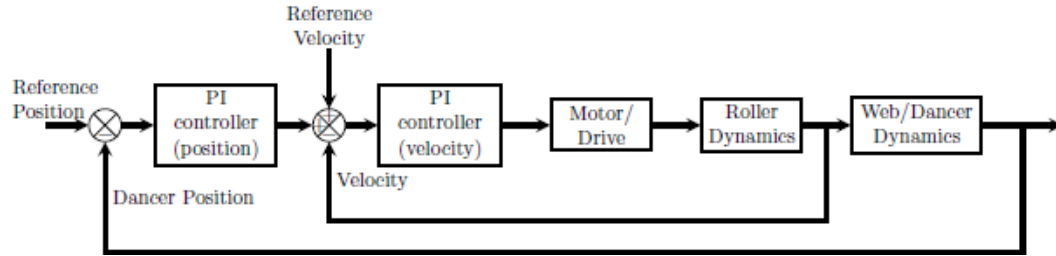


Figure 3 – Speed based web tension control system using dancer position feedback

The design of a control system for a web line involves determining the control structure and the corresponding parameters. This paper assumes that a Proportional + Integral controller structure is used for all five speed loops and for the tension loops at the unwind and rewind. The next step in design is determining the proportional and integral gains for each controller. A systematic method for determining the gains in the seven controllers is the focus of this paper.

Model Order Reduction

Hutton demonstrated a Routh Approximation (RA) method for approximating a third order or higher transfer function with a lower order transfer function that retains the same initial response and stability of the original transfer function in [10] and [11]. Figure 4 shows the Bode plot of a dynamic system with a third-order transfer function and its second-order approximation using this method. The Routh Array was originally described in [12], but is now in many textbooks, e.g. [13].

Performance Goals

Parameters of a second-order response that are immediately apparent to the user are damping ratio, ζ , and rise time, t_r . The damping ratio defines if a perturbed system does not oscillate ($\zeta \geq 1.0$) or oscillates ($0 = \zeta < 1.0$) and how quickly the oscillation dies out. Rise time is defined as the amount of time required for the output of the system to rise from 0% to 100% of its final value (Palm also notes that some writers define rise time as the time for the step response to go from 10% to 90% of the final value) [14]. For values of ζ such that $0.1 \leq \zeta \leq 0.9$, the natural frequency of a second order system is related to rise time by

$$\omega_{nat} = \frac{\pi - \tan^{-1}\left(\frac{\sqrt{1-\zeta^2}}{\zeta}\right)}{t_r \sqrt{1-\zeta^2}} \quad \{1\}$$

where ω_{nat} is the natural frequency of the system in rad/sec, and t_r is the rise time in seconds. For values of $\zeta > 0.9$, the inverse tangent becomes asymptotic.

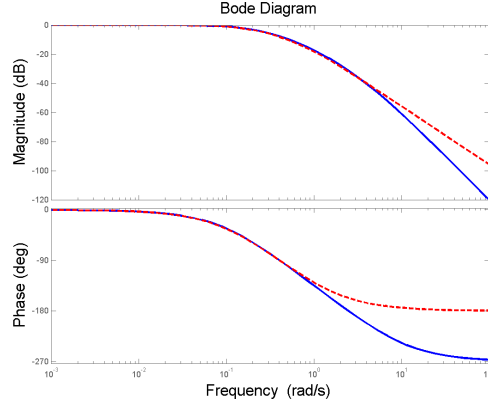


Figure 4 – Bode plot of an example third-order transfer function (blue) and its second-order approximation (red dashed) obtained using the RA method. The approximate transfer function tracks the third-order one well up to about 4 rad/s.

SYSTEM MODELING

The motor is modeled as a first-order linear differential equation with constant parameters as shown in Eqn. {2}.

$$J_n \dot{\omega}_n = -(B_{fn} + C_{mn})\omega + K_{mn}u_n + R_n T_n / G R_n \quad \{2\}$$

The Laplace transform of {2} leads to the open loop transfer function from current input, u_n , to motor speed, ω_n , given in Eqn. {3}.

$$G_1(s) = \frac{\Omega_n(s)}{U_n(s)} = \frac{K_{mn}/J_n}{s + (B_{fn} + C_{mn})/J_n} \quad \{3\}$$

A physical model of the free span of the web is shown in Figure 5. It is assumed that the web is linear-elastic, has a constant cross sectional area, undergoes small strains, and does not slip on the idle rollers. With these assumptions from [15], the following nonlinear differential equation results from a combination of the law of conservation of mass for the control volume and the application of Hooke's Law

$$L_n \frac{dT_n}{dt} = EA(v_{n+1} - v_n) + (v_n t_{n-1} - v_{n+1} t_n) \quad \{4\}$$

where t_n is the tension in the span of interest, v_n is the roller speed of the roller at the entering end of the span, v_{n+1} is the speed at the outgoing end of the span, and t_{n-1} is the tension in the previous span. Equation {4} is nonlinear because of the multiplication of

roller speed and span tension. This equation can be linearized if it is assumed that all variables (t_n and v_n) undergo small changes about initial steady-state values. The result is

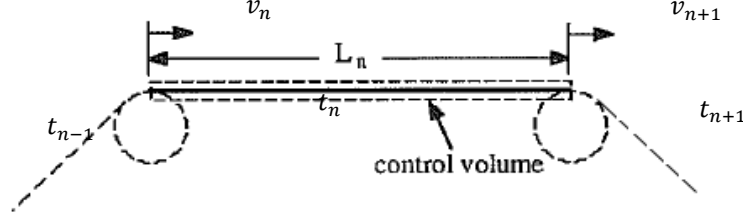


Figure 5 – The free span is the material between the points of contact with the end rollers that experiences tension and velocity.

$$L_n \frac{dt_n}{dt} = EA(v_{n+1} - v_n) + (V_{n,0}t_{n-1} - V_{n+1,0}t_n) \quad \{5\}$$

where $V_{n,0}$ and $V_{n+1,0}$ are the steady-state velocity of the web at the incoming and outgoing rollers. Equation {5} may be used to demonstrate behavior of the span tension in the steady-state operation (i.e., $(dT_n/dt) = 0$). The tension in a span is dependent on the difference in the velocities at the ends of the web, and that tension is transferred from an upstream span to a downstream span.

The Laplace transform of Eqn. {5}, leads to the open loop transfer function relating the web velocity at the incoming roller to web span tension given in Equation {6}. The negative sign is for the situation where the driven roll is upstream of span n .

$$\frac{T_n(s)}{V_n(s)} = \frac{(-EA/L_n)}{s + (V_{n+1,0}/L_n)} \quad \{6\}$$

The dancer (see Figure 6) is modeled with summation of moments about the dancer pivot with the dancer angle, γ , increasing away from the spans. The differential equation is

$$\frac{d\dot{\gamma}}{dt} = \frac{f_{qn}}{J_{pn}} - T_n \frac{(L_{arm} - R_n)}{J_{pn}} - T_{n-1} \frac{(L_{arm} + R_n)}{J_{pn}} - \frac{C_{pn}}{J_{pn}} \dot{\gamma} - \frac{K_{pn}}{J_{pn}} \gamma + \frac{m_p g l_{cg}}{J_{pn}} \sin \gamma \quad \{7\}$$

where K_{pn} is the spring constant of the dancer and C_{pn} is the damping in the pivot of the dancer arm and torque application system, m_p is the mass of the pendulum dancer, l_{cg} is the distance from the pivot to the center of gravity, and g is the gravitational constant. This equation can be linearized if it is assumed that the input torque (f_{qn}), outgoing span tension (T_n), and the initial conditions for the dancer position are all zero, and that the small angle approximation applies ($\sin \gamma \approx \gamma$). With these assumptions, the Laplace Transform of the linearized version of Eqn. {7} leads to an open loop transfer function relating the tension in the incoming span ($T_{n-1}(s)$) to the dancer position ($\Gamma(s)$).

$$\frac{\Gamma(s)}{T_{n-1}(s)} = \frac{(L_{arm} + R_n)/J_{pn}}{(s^2 + (C_{pn}/J_{pn})s + (K_{pn} + m_p g l_{cg}/J_{pn}))} \quad \{8\}$$

Eqn. {8} includes the restorative moment due to gravity ($m_p g l_{cg} \sin \gamma$) which ensures that the dancer system is not a pure integrator if there is no damping or spring constant assumed in the system.

GAIN CALCULATION METHOD

This method assumes that the S-wrap and pull roll motors are under pure speed control, and that the unwind and rewind rolls are under speed-based tension control. Since there is a speed control loop in both cases, the proportional and integral gains for all five speed loops are found first. Then the gains for the tension loops are found.

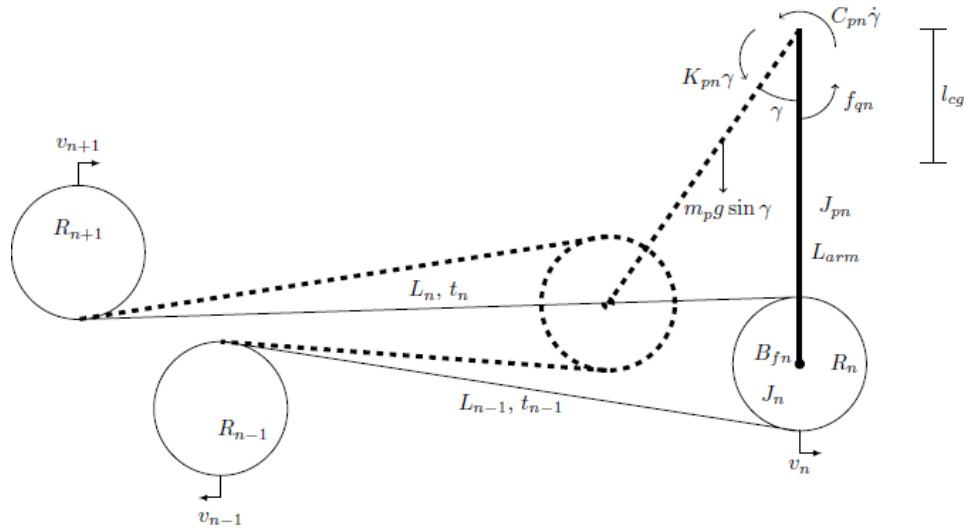


Figure 6 – A physical model of dancer subsystem showing variables and physical parameters

Speed Control

There are five speed control systems in the Euclid Web line. Equation {3} can be used as the open loop transfer function for each speed control system. A PI velocity controller is placed in series with transfer function in Eqn. {3}, and the loop is closed. The output speed of the motor is compared with the speed reference. The block diagram in Figure 7 shows the speed loop where the speed feedback is the motor shaft speed.

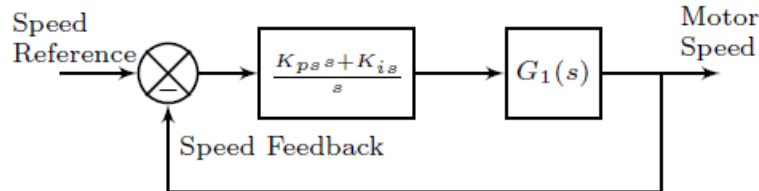


Figure 7 – The closed-loop block diagram from the speed reference to the motor speed with PI control.

The closed loop transfer function relating the motor speed reference to the motor speed is

$$\frac{\Omega_n(s)}{\Omega_{ref}(s)} = \frac{K_{mn}/J_n (K_{ps}s + K_{is})}{s^2 + \left(\frac{B_{fn} + C_{mn}}{J_n} + \frac{K_{mn}}{J_n} K_{ps}\right)s + \frac{K_{mn}}{J_n} K_{is}} \quad \{9a\}$$

Or in terms of a natural frequency and damping ratio

$$\frac{\Omega_n(s)}{\Omega_{ref}(s)} = \frac{K_{mn}/J_n (K_{ps}s + K_{is})}{s^2 + 2\zeta\omega_{nat}s + \omega_{nat}^2} \quad \{9b\}$$

Equation {9a} defines a second order linear system. The gains are displayed in the closed loop transfer function. The motor can be driven to a specific speed with the desired performance through the selection of a damping ratio, ζ , and a rise time, t_r . Equation {1} can be used to calculate the natural frequency. The PI controller gains for each speed control may be calculated from equations that result from comparing the characteristic equations (from {9a} and {9b}).

$$K_{is} = \frac{J_n \omega_{nat}^2}{K_{mn}} \quad \{10\}$$

$$K_{ps} = \left[2\zeta\omega_{nat} - \frac{B_{fn} + C_{mn}}{J_n} \right] \frac{J_n}{K_{mn}} \quad \{11\}$$

where K_{is} is the integral gain and K_{ps} is the proportional gain for the speed control system. The gains for each of the five speed control systems can be found from these equations with the associated parameters inserted.

Tension or Position Control

Figure 2 shows tension control with load cell feedback, and Figure 3 shows tension control with dancer position feedback. There are two sets of Proportional and Integral gains in each system. Determination of the PI gains for the tension loop is difficult because the open loop system from reference speed to span tension is at least third order, if not higher. And after a PI controller is added, the closed loop system relating motor speed to the speed reference is fourth order, if not higher.

In either case, the speed loop needs to be closed first, and then the closed loop transfer function relating the reference velocity of the motor to its output velocity determined. The transfer function is Eqn. {9} or

$$G_s(s) = \frac{R_n \Omega_n(s)}{R_n \Omega_{ref}(s)} = \frac{V_n(s)}{V_{nref}(s)} = \frac{\left(\frac{K_{ps}s + K_{is}}{s}\right) G_1(s)}{1 + \left(\frac{K_{ps}s + K_{is}}{s}\right) G_1(s)} \quad \{12\}$$

$G_1(s)$ refers to Eqn. {3}, the open loop transfer function relating motor input current to motor speed. $G_s(s)$ is the closed loop transfer function relating motor speed to motor speed reference.

When load cell feedback is used to adjust the speed reference of the motor, the transfer function for the open loop plant is the combination of Eqn. {12} and the transfer function relating incoming roller velocity to span tension, Eqn. {6}, if the load cell is the first idle roller in the web line after the unwinding motor. Figure 8 shows the open-loop

block diagram from reference speed to span tension. The “conv.” block is a conversion factor made up of the gear ratio and the unwind roll radius to convert from motor angular speed to web linear speed. The open-loop transfer function shown in Figure 8 is third-order if there is only one span between the unwind roll and the load cell. While that is the ideal case, sometimes more spans are required due to space constraints in the layout of the line. If that happens, the order of the system increases by 2 with each additional idler and span.

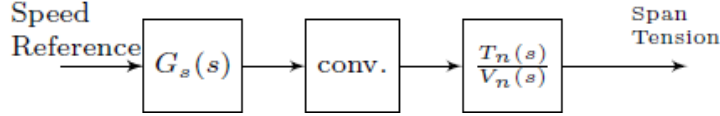


Figure 8 – The open-loop block diagram from reference speed to span tension. The "conv." block converts the motor speed to web speed. The open-loop transfer function in the third block is given in Eqn. {6} in terms of parameters .

The best case is that the open loop transfer function in Figure 8 is third order, but this is not the case for the unwind section of the Euclid Web Line. The minimum order would be 5th order, but it is more than that if all the idle rollers and spans between the unwind roll and the load cell. But, the high order system can be reduced by assuming that the dissipative nature of the idlers can be ignored, and by treating all the spans from the unwind to the load cell as one span with a length equal to the sum of the lengths of all the spans. Combining the spans into one reduces the order of the model to third order for the open-loop load cell control. The transfer function shown in Figure 8 is called $G_2(s)$ once it is simplified. The transfer function has the form shown in Eqn. {13}.

$$G_2(s) = \frac{b_1 s^m + \dots + b_{m+1}}{s^n + a_1 s^{n-1} + \dots + a_n} \quad \{13\}$$

When dancer position feedback is used to adjust the reference speed, the block diagram of the open-loop system is shown in Figure 9 where all the parts just discussed for load cell feedback exist, but one more transfer function is added. Equation. {8} is the transfer function relating incoming span tension to dancer position. If the dancer roller is the first roller the web encounters after being unwound, the combined open-loop transfer function is fifth-order. If the dancer is not the first idler the web encounters, then the order of the system is increased by two. Ignoring the dissipative effects of the additional idlers and summing the length of the spans together into one span will reduce the order back to fifth order. The combined transfer function shown in Figure 9 can be simplified and put in the form of Eqn. {13}.

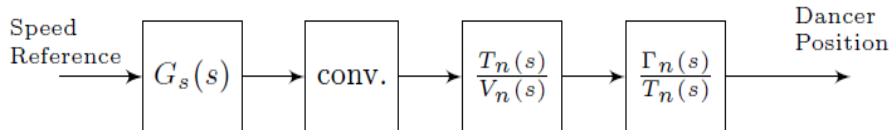


Figure 9 – The open-loop block diagram from reference speed to dancer position. This whole transfer function is $G_2(s)$.

Approximating the Transfer Function

The Routh Approximation (RA) method is now used to reduce the characteristic polynomial ($G_2(s)$) from third-order in the case of load cell feedback or fifth-order for dancer position feedback to second-order ($\tilde{G}_2(s)$) as shown in Figure 10. With the open loop approximated as $\tilde{G}_2(s)$, the gains for the PI controller in the closed loop system (Eqn. {15}) can be found by assuming a real pole exists and simultaneously solving a system of equations (Eqns. {17} and {18}). The closed loop system block diagram is shown in Figure 11.

The RA method will take in the open-loop tension transfer function, $G_2(s)$, of the modeled system as a numerator vector of coefficients, $[b_1 \ b_2 \ ... \ b_{m+1}]$ and a denominator vector of coefficients, $[1 \ a_1 \ ... \ a_n]$ (see Eqn. {13}). The RA method output is a set of two vectors, M_n and M_d , which make up the approximated transfer function $\tilde{G}_2(s)$. The form for a second order approximation is

$$\tilde{G}_2(s) = \frac{M_n(2)s + M_n(3)}{s^2 + M_d(2)s + M_d(3)} \quad \{14\}$$

which is then included in the closed loop transfer function with the PI controller, $G_3(s)$,

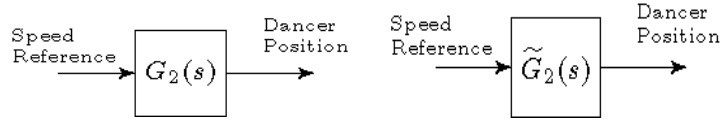


Figure 10 – For Dancer position feedback, the Routh Approximation method reduces the open-loop transfer function $G_2(s)$ to $\tilde{G}_2(s)$.

$$G_3(s) = \frac{\left(\frac{K_{pt}s + K_{it}}{s}\right)\tilde{G}_2(s)}{1 + \left(\frac{K_{pt}s + K_{it}}{s}\right)\tilde{G}_2(s)} \quad \{15\}$$

and compared with the desired characteristic polynomial, $G_{3d}(s)$, below.

$$G_{3d}(s) = \frac{(K_{pt}s + K_{it})(M_n(2)s + M_n(3))}{(s + k_r\zeta\omega_{nat})(s^2 + 2\zeta\omega_{nat}s + \omega_{nat}^2)} \quad \{16\}$$

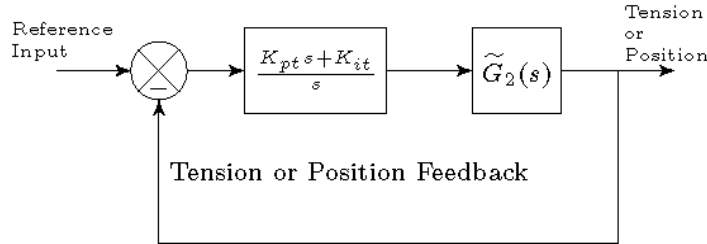


Figure 11 – The closed-loop block diagram for tension or position control incorporating the approximated transfer function from the RA method.

Once Eqn. {15} is simplified, its coefficients may be equated to those of the desired transfer function in Eqn. {16} which yields the following set of simultaneous equations ({17} and {18}).

$$k_r \omega_{nat} \zeta - K_{pt} M_n(2) = -2\zeta \omega_{nat} + M_d(2) \quad \{17\}$$

$$k_r \left(2\zeta^2 \omega_{nat}^3 - \frac{M_n(2)}{M_n(3)} \zeta \omega_{nat}^3 \right) - K_{pt} M_n(3) = -\omega_{nat} + M_d(3) \quad \{18\}$$

After solving the above set of equations for k_r and K_{pt} , the integral gain is found by

$$K_{it} = \frac{k_r \omega_{nat}^3 \zeta}{M_n(3)}. \quad \{19\}$$

If k_r is large enough, the effect of the associated pole is small compared to that for the two complex roots [13]. But in the case of applying the method to the Euclid Line, the magnitude of k_r has generally been small and the effect is not small. The numerator constant, $M_n(3)$, from the approximated transfer function, $\widetilde{G}_2(s)$, is in the denominator of Eqn. {19} which means that large magnitudes in the numerator will force small integral gains which can be problematic.

SYSTEMATIC METHOD FOR DETERMINING CONTROLLER GAINS

First, determine the physical parameters of the web line by calculation or measurement. These include the motor inertia, the motor damping, the motor constant, the roller inertias, the gear ratio between each motor and the spindle that contacts the web, roller bearing friction values, roller radii, span length between rollers, Young's modulus for the web, cross-sectional area of the web. If there is a dancer, determine the type of dancer, arm length (if it is a pendulum style), the dancer's mass and inertia, and applied torque (pendulum) or force (translational). Determine the steady-state operating web speed for the line.

Divide the web line into control sections, the number of which may be different than the number of motors in the web line. These sections should break at driven rollers and can be either speed controlled or speed-based tension controlled. For each section, develop a model for the motor speed loop, and if a tension feedback loop or position feedback loop exists, develop a model that relates the motor speed to the tension (measured by a load cell) or dancer position.

Select a rise time, t_r , and damping ratio, ζ , for each motor and tension or position control loop. These can be the same throughout or specific to each loop and each motor.

Once the models for the motor speed loops are created for each control section in the web line, use Eqns. {10} and {11} to determine the related gains. Then create the closed-loop transfer function for the speed loop, $G_1(s)$, and place it in series with the transfer function for the span tension (Eqn. {6}) or dancer position (Eqn. {8}) making $G_2(s)$. Combine and simplify the transfer functions. Then reduce the order of the transfer function using the Routh Approximation Method making $\widetilde{G}_2(s)$. Once the reduced order transfer function is known, Eqns. {17} and {18} can be simultaneously solved, and substituted into Eqn. {19} to determine the tension or position control loop gains.

The next step is to apply the gains to the web line. Caution should be taken in this step. Once the gains are applied, enable the line and then apply tension only. Watch the tension feedback and observe that the tension behaves as expected. If the tension display or dancer position oscillates, the tension loop or position loop gains need to be increased. The gains found by this method are found using several assumptions including linear materials and that the idle rollers can be ignored. Therefore, consider the calculated gains to be a starting point in tuning the speed-based tension controllers in the line. Once the

tension display is stable, try a ramp up to about 20% of the operating speed. Watch the web spans to see if they vibrate or go slack. Watch the tension display. These will inform the decision to leave the gains as they are or to adjust them more.

THE SYSTEMATIC METHOD APPLIED TO THE EUCLID WEB LINE

The Euclid Web Line at Oklahoma State University's Web Handling Research Center was used to evaluate the systematic method. The physical parameters collected from the line are tabulated in Tables 3 through 6 in the Appendix. Figure 1 shows the Euclid Web Line control sections. The unwind section is the unwind roll on the left up to the S-wrap Lead (roll 10), the S-wrap section is between rolls 10 and 11, the process section is from the S-wrap Follow (roll 11) to the pull roll (roll 17), and the rewind section is from the pull roll to the rewind roll on the far right. The unwind and rewind sections have an outer-loop feedback while the S-wrap and process sections are under pure speed control.

Following the process laid out in the previous section, a model for each control section needs to be created. Equation {3} is the speed control model for each of the five motors. Multiplying both sides of Eqn. {3} by $R_n GR_n$ will convert the equation to tangential speed of the roll instead of angular velocity of the motor. A rise time of 0.3 seconds and a damping ratio of 0.9 were selected for the example in this paper. The same rise time and damping ratio are used for each controller in the web line. Using Eqn. {1}, the natural frequency of the control loop is 20.6 rad/s . The inertia, J_1 , is calculated by reflecting the motor inertia, J_{m1} , through the gear ratio, GR_1 , to the shaft where the web is and adding it to the shaft and wound web inertia, J_{s1} . Eqns. {10} and {11} are used after selecting a rise time and damping ratio to calculate the proportional and integral gains for the speed loops which are shown in Table 1.

The unwind section has 3 different feedback devices: a dancer, a load cell at roller 3, or a load cell at roller 9. The rewind section has a load cell at roller 19. The process for creating the model of the unwind section with dancer position feedback follows. Convert the motor model (Eqn. {3}) and the speed control into a transfer function using Eqn. {12} ($G_s(s)$) with the unwind parameters. Then $G_s(s)$ is simplified. Form $G_2(s)$ by placing $G_s(s)$ in series with two more transfer functions which are Eqn. {6} (the incoming roller speed to span tension model) and Eqn. {8} (the incoming span tension to dancer displacement model) (see Figure 9). The lumped span model is assumed so the span length, L_n , in Eqn. {6} is $L_n = L_1 + L_2 + L_3$ or 5.079 ft . Transfer functions in series multiply. Eqn. {12} is multiplied by Eqn. {6} and Eqn. {8}. Once $G_2(s)$ simplified, the coefficients are processed by the Routh Approximation Method and the proportional and integral gains are calculated by solving Eqns. {17}, {18}, and Eqn. {19}. Repeat this process with the rewind section where a load cell is used. Form $G_2(s)$ with Eqn. {6} in series with Eqn. {12} for the rewind. Table 2 shows the proportional and integral gains for the unwind and rewind sections determined following this method using a damping ratio of 0.9 and a rise time of 0.3 seconds.

Motor & Type of control		Kp	Ki
Unwind	Speed	2.7928	16.1576
S-Wrap Lead	Speed	5.5421	32.0624
S-Wrap Follow	Speed	5.5421	32.0624
Pull Roll	Speed	5.9853	34.6265
Rewind	Speed	3.91	22.697

Table 1 – Motor speed gains found using the process with a damping ratio of 0.9 and a rise time of 0.3 seconds.

Section & Type		Kp	Ki
Unwind	Position	1.0694	0.6054
Rewind	Tension	0.3475	0.0003101

Table 2 – Position and tension control gains for the unwind and rewind sections.

EXPERIMENTAL STUDY

The Euclid Web Line was exercised after applying the gains calculated in the previous section. The gains calculated using the method in the previous section are expecting feedback errors in base units. This implies that the speed loop gains expect speed errors in ft/s. The tension loop gains expect errors in pounds. The dancer position gains are calculated for errors in radians. If those units are not the units used in the web line control and feedback system, the gains must be converted into the correct units. The Euclid Web Line used RPM for the speed loops, percent of maximum load in the tension loop, and degrees in the dancer position loop.

The Euclid Web line was exercised through a 400 FPM start up procedure following an industrial S-curve reference twice using the 0.3 second rise time and 0.9 damping ratio. The load cell at roller #3 was used for feedback in the unwind section. The rewind section only had load cell feedback. Figure 12 shows the speed tracking performance on the left and the tension tracking performance on the right. The proportional gain in the tension loop for the unwind was increased by 10 to obtain better performance. The rewind section proportional gain was also increased by 10 fold to obtain better reference tracking, but little change in performance was noted.

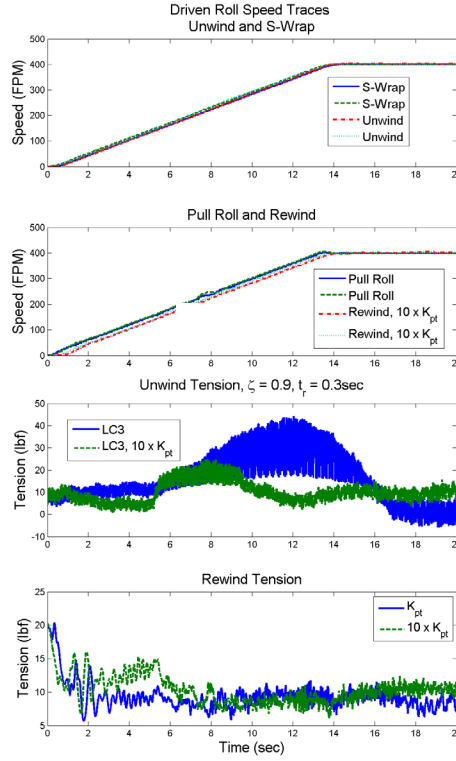


Figure 12 – The left plot shows speed tracking performance of the unwind and s-wrap (above), and the pull roll and rewind motors (below) during a 400 FPM start up following an industrial S-curve with $\zeta = 0.9$ and $t_r = 0.3$ seconds. Load cell #3 was the feedback device for the unwind section. The proportional gain for the unwind tension was increase 10 fold to obtain better performance. The K_{pt} gains for the rewind section were also increased by 10 fold but the performance is similar during most of the operation. Only during the first few seconds are the two records different.

The unwind section of the Euclid Web Line was switched to dancer position feedback and the 400 FPM start up procedure using an industrial S-curve was accomplished. Figure 13 shows the speed tracking performance for the unwind and rewind sections on the left, and the figure shows the rewind tension and dancer position on the right. The dancer position had a larger magnitude of oscillation before multiplying the proportional gain by 10. There was no change in the rewind tension performance because the proportional gain was increased 10 fold in both cases.

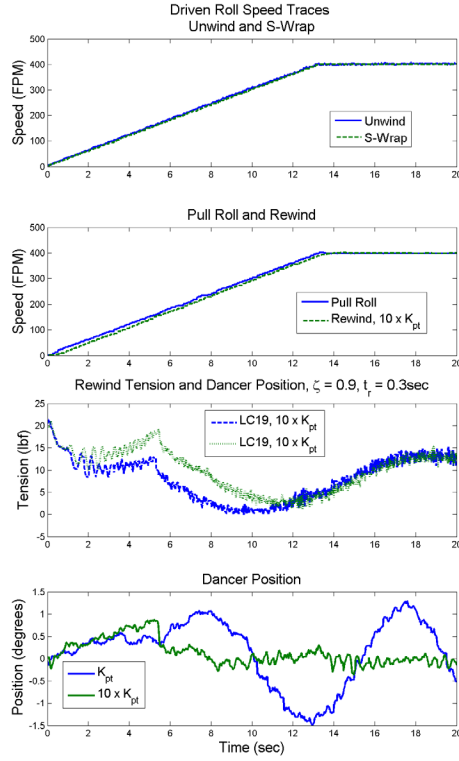


Figure 13 – The Euclid line with dancer feedback control of the unwind section goes through a 400 FPM start up procedure following an industrial S-curve reference. The rewind gains were unchanged between runs and similar performance was recorded for both runs. The unwind proportional gain for the dancer position was increased 10 fold to obtain better position tracking.

CONCLUSION

This paper has presented a systematic method for determining the controller gains for a web handling line. The gains are found under the assumptions of linear models, linearly elastic web materials, idle rollers may be neglected, and that second order model approximations will work in place of higher-order models. Gains were calculated for the Euclid Web line following the method in this paper. Seven sets of PI gains were determined. Experimental studies on the Euclid Web Line with the calculated gains were found to be good for the speed loops, but were not successful for the tension loops. Successful performance could be obtained if the proportional gains in the tension loops was increased. Even though the gains determined may not be unique and fully optimal, they provide a good starting point for tuning a line after it is built or after a major change is made in the line.

REFERENCES

- [1] J. Damour, *The Mechanics of Tension Control*, Wind Gap, PA: Converter Accessory Corporation, 2004, pp. 1-29.
- [2] D. P. Campbell, *Dynamic Behavior of the Production Process: Process Dynamics*, P. S. Buckley, Ed., New York, NY: John Wiley & Sons, Inc., 1958.
- [3] D. King, "The mathematical model of a newspaper press," *Newspaper Techniques*, vol. 1, pp. 3-7, 1969.
- [4] K. P. Grenfell, "Tension control paper-making and converting machinery," *IEEE Transactions on Applications and Industry*, vol. 83, pp. 234-240, 1964.
- [5] G. Brandenburg, "New mathematical models for web tension and register error," in *Proc. 3rd International IFAC Conf. on Instrumentation and Automation in the Paper, Rubber, and Plastics Industries*, Brussels, 1976.
- [6] J. J. Shelton, "Dynamics of web tension control with velocity or torque control," in *American Control Conference, 1986*, 1986.
- [7] K.-H. Shin, "Distributed control of tension in multi-span web transport systems," Ph.D. thesis, Oklahoma State University, Stillwater, OK 1991.
- [8] K. N. Reid and K. H. Shin, "Variable-Gain Control of Longitudinal Tension in a Web Transport System," in *Proc. of the 1st International Conference on Web Handling (IWEB 1991)*, Stillwater, 1991.
- [9] P. R. Pagilla, *Web Handling Seminar*, 2017, p. Tab 4.
- [10] M. Hutton and M. J. Rabins, "Simplification of High-Order Mechanical Systems Using the Routh Approximation," *Journal of Dynamic Systems, Measurement, and Control*, vol. 97, pp. 383-392, 12 1975.
- [11] M. Hutton and B. Friedland, "Routh Approximations for Reducing Order of Linear, Time-Invariant Systems," *IEEE Trans. on Automatic Control*, Vols. AC--20, pp. 329-337, 6 1975.
- [12] E. J. Routh, *A Treatise on the Stability of a Given State of Motion, Particular Steady Motion*, London: Macmillan & Co., 1877.
- [13] R. Dorf, *Modern Control Systems*, Upper Saddle River, N.J: Pearson Prentice Hall, 2011.
- [14] W. Palm, *System Dynamics*, New, York: McGraw-Hill, 2014.
- [15] K. N. Reid and K. -C. Lin, "Control of Longitudinal Tension in Multi-Span Web Transport Systems During Start-up," *Proceedings of the Second International Conference on Web Handling*, pp. 77-95, June 1993.

APPENDIX

Parameter	Value	Units
Motor Inertia	4.786E-02	slug-ft ²
Gear Ratio	2.635E-01	shaft rotations per motor rotation
Shaft inertia	3.680E-01	slug-ft ²
Roller inertia	4.635E-03	slug-ft ²
Inertia of wound web (14in dia.)	5.300E-02	slug-ft ²
Bearing Friction	6.073E-04	lbf-ft-s
Motor Damping	0.000E+00	lbf-ft-s
Motor Constant	1.274E+01	lbf-ft/A
Roller radius	1.250E-01	ft
Young's modulus (Tyvek)	6.667E+06	lbf/ft ²
Web cross-sectional area	2.262E-04	ft ²
Span Length	5.079E+00	ft
Steady-state speed	6.667E+00	ft/s
Dancer Arm Length	1.327E+00	ft
Dancer Inertia	2.090E-01	slug-ft ²
Dancer applied torque	1.845E+01	lbf-ft

Table 3 – Physical parameters used in the example for the unwind section

Parameter	Value	Units
Motor Inertia	4.072E-02	slug-ft ²
Gear Ratio	7.168E-02	shaft rotations per motor rotation
Shaft inertia	1.315E+00	slug-ft ²
Bearing Friction	6.073E-04	lbf-ft-s
Motor Damping	0.000E+00	lbf-ft-s
Motor Constant	6.249E+01	lbf-ft/A
Roller radius	5.000E-01	ft

Table 4 – Physical parameters for the S-Wrap.

Parameter	Value	Units
Motor Inertia	4.072E-02	slug-ft ²
Gear Ratio	7.766E-02	shaft rotations per motor rotation
Shaft inertia	4.686E-01	slug-ft ²
Bearing Friction	6.073E-04	lbf-ft-s
Motor Damping	0.000E+00	lbf-ft-s
Motor Constant	3.090E+01	lbf-ft/A
Roller radius	2.500E-01	ft

Table 5 – Physical parameters for the Pull Roll

Parameter	Value	Units
Motor Inertia	4.786E-02	slug-ft ²
Gear Ratio	2.635E-01	shaft rotations per motor rotation
Shaft inertia	3.680E-01	slug-ft ²
Inertia of wound web (14in dia.)	3.900E-02	slug-ft ²
Bearing Friction	6.073E-04	lbf-ft-s
Motor Damping	0.000E+00	lbf-ft-s
Motor Constant	1.274E+01	lbf-ft/A
Roller radius	1.250E-01	ft
Young's modulus (Tyvek)	6.667E+06	lbf/ft ²
Web cross-sectional area	2.262E-04	ft ²
Span Length	1.141E+01	ft
Steady-state speed	6.667E+00	ft/s

Table 6 – Physical parameters for the rewind